

# Highly Oriented Nanofibrils of Regioregular Poly(3-hexylthiophene) Formed via Block Copolymer Self-Assembly in Liquid Crystals

Xia Tong, Dehui Han, Daniel Fortin, and Yue Zhao\*

**A novel method making use of block copolymer self-assembly in nematic liquid crystals (LCs) is described for preparing macroscopically oriented nanofibrils of  $\pi$ -conjugated semiconducting polymers. Upon cooling, a diblock copolymer composed of regioregular poly(3-hexylthiophene) (P3HT) and a liquid crystalline polymer (LCP) in a block-selective LC solvent can self-assemble into oriented nanofibrils exhibiting highly anisotropic absorption and polarized photoluminescence emission. An unusual feature of the nanofibrils is that P3HT chains are oriented along the fibrils' long axis. This general method makes it possible to use LCs as an anisotropic medium to grow oriented nanofibrils of many semiconducting polymers insoluble in LCs.**

## 1. Introduction

Much research effort has been devoted to preparing nanofibers or nanowires of  $\pi$ -conjugated semiconducting polymers due to many potential applications making use of their anisotropic optical or charge transfer properties.<sup>[1–3]</sup> Polythiophenes are one of the most studied classes of semiconducting polymers and various methods have been developed to obtain their one-dimensional nanostructures. These include epitaxial growth in solution with long needles of a molecular crystal,<sup>[4]</sup> solvent-induced aggregation,<sup>[5–8]</sup> polymerization in solution with sacrificial seeds,<sup>[9]</sup> electrospinning,<sup>[10]</sup> dip-pen nanolithography<sup>[11]</sup> and block copolymer self-assembly.<sup>[12,13]</sup> However, it remains challenging to prepare oriented nanofibers on a macroscopic scale. Most of the existing methods are unable to do this. For instance, aggregation of polythiophenes in solution can produce crystalline nanowires. Although each single nanowire contains ordered polymer chains and is highly anisotropic, the many nanowires in a sample are randomly oriented from each other and, thus, no macroscopic anisotropic properties can be obtained. In the case of block copolymer self-assembly in bulk, rod-like nanodomains of polythiophenes can be formed via microphase separation, but there is no polymer chain orientation along or normal to the nanodomains' long axis.<sup>[14]</sup> Few reported methods allow one to prepare

macroscopically oriented nanofibers of polythiophenes. To this regard, a report of Samitsu et al. is of particular interest.<sup>[15]</sup> By dissolving a polythiophene, namely, poly(3,3'-didodecylquaterthiophene) (PQT12) in a nematic liquid crystal (LC) oriented by rubbed surfaces, polythiophene chains can align in the same direction as LC molecules and, on cooling, aggregate into nanofibers growing in the direction of  $\pi$ - $\pi$  stacking of thiophene chains. Similar to the nanowires formed by aggregation in solution, the resulting nanofibers are perpendicular to the LC director, i.e., normal to the chain axis of the semiconducting

polymer. Although interesting, the generality of this method is limited because it is applicable only to polythiophenes initially soluble in the LC solvent, while many, such as the most exploited poly(3-hexylthiophene) (P3HT), cannot be used due to their insolubility in LCs.<sup>[15]</sup>

In this paper, we demonstrate, for the first time, that block copolymer (BCP) self-assembly using nematic LCs as a block-selective solvent may provide a general means for preparing macroscopically oriented nanofibrils of polythiophenes that are insoluble in LCs. The idea is to use a diblock copolymer comprised of a LC-insoluble (or LC-phobic) polythiophene and a LC-soluble (or LC-philic) liquid crystalline polymer (LCP). Similar to amphiphilic BCPs in water, when such a polythiophene-LCP BCP is dissolved in a LC solvent, self-assembly with polythiophene chains tending to aggregate could take place under certain conditions. Indeed, using a BCP containing regioregular P3HT, we found that self-assembly in oriented nematic LCs could give rise to macroscopically oriented nanofibrils of the semiconducting polymer, with an unusual feature that P3HT chains are oriented parallel to the long axis of fibrils. These oriented nanofibrils display highly anisotropic absorption and polarized photoluminescence emission. The likely mechanism, driven by the BCP self-assembly in oriented LC solvents, is discussed. We emphasize that this new method is for orienting P3HT, not for oligothiophenes for which there are also many reports in the literature.<sup>[16–19]</sup>

X. Tong, Dr. D. Han, Dr. D. Fortin, Prof. Y. Zhao  
Département de chimie  
Université de Sherbrooke  
Sherbrooke, Québec, Canada J1K 2R1  
E-mail: Yue.Zhao@Usherbrooke.ca



DOI: 10.1002/adfm.201202056

## 2. Results and Discussion

We used a diblock copolymer comprising regioregular P3HT and a side-chain LCP bearing azobenzene mesogens.

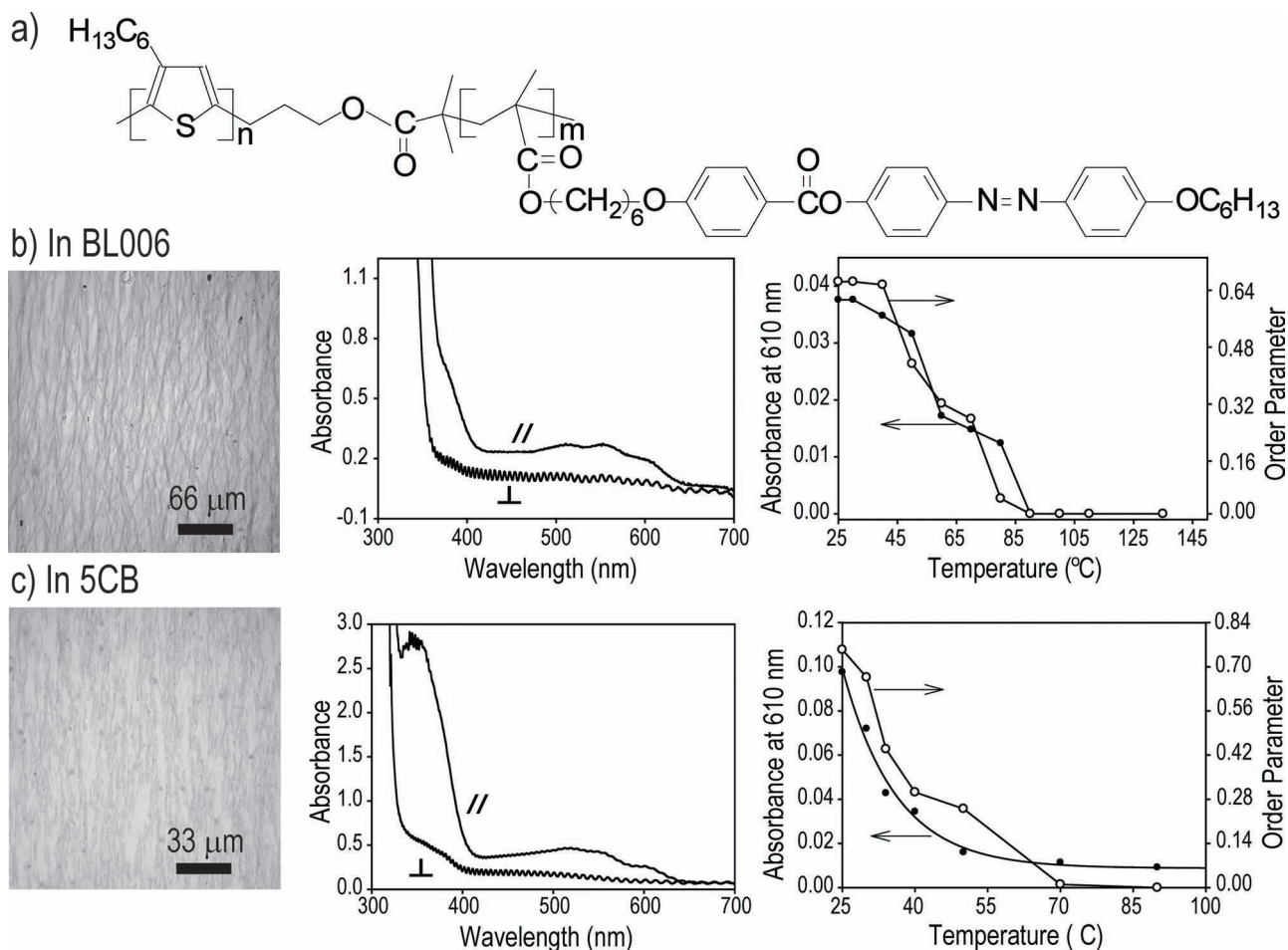


**Figure 1.** Chemical structure of the diblock copolymer P3HT-*b*-PAzoMA (a) and its macroscopically oriented nanofibrils self-assembled in BL006 (b) and 5CB (c). Left: bright-field photomicroscopy image; middle: polarized absorption spectra at room temperature with incident beam polarized parallel and perpendicular, respectively, to the cell rubbing direction; and right: changes in absorbance of the absorption band at 610 nm as well as order parameter calculated from polarized spectra at this wavelength as a function of temperature on cooling. The block copolymer concentration was 2 wt% in BL006 and 4 wt% in 5CB.

The chemical structure of the sample, P3HT<sub>43</sub>-*b*-PAzoMA<sub>120</sub>, is given in **Figure 1a** and its synthesis was reported previously.<sup>[14]</sup> Two commercially available nematic LCs, namely, 5CB and BL006 (from Merck), were chosen for the BCP self-assembly. While 5CB is a single-component LC (4,4'-pentylcyanobiphenyl) with a nematic to isotropic phase transition (clearing) temperature  $T_{\text{ni}} \approx 35$  °C, BL006 is a eutectic mixture with a much higher  $T_{\text{ni}}$  at about 116 °C. To mix the BCP with either 5CB or BL006, the two components were first dissolved by a small amount of chloroform (about 0.5 mL for 100 mg of the LC) to ensure the homogeneity of the mixture; after drying, the mixture was heated to 130 °C (isotropic phase) and flow-filled into a 10  $\mu\text{m}$ -gap glass cell with parallel rubbed polyimide surfaces. The sample was finally cooled slowly from the isotropic phase to room temperature at a rate of  $\approx 1$  °C/min to induce the self-assembly process. Unless otherwise stated, all measurements or observations were made with the sample inside the glass cell under ambient conditions.

Figure 1 presents two sets of results obtained with 2 wt% of BCP in BL006 (Figure 1b) and 4% of BCP in 5CB (Figure 1c).

In both cases, shown on the left is a bright-field photomicroscopy image, in the middle are polarized UV-vis absorption spectra and, on the right, are plots of the absorbance of the 610 nm band and the order parameter calculated from this band vs. temperature on cooling the sample from the isotropic state to room temperature. Several observations and analyses can be made. First, with the two different LCs as host, when a homogeneous mixture is cooled to room temperature, highly oriented fibrils of the BCP are formed as revealed by the photomicrographs. The fibrils are oriented along the rubbing direction, i.e., in the same direction as LC molecules. Secondly, the absorption spectra recorded with the spectrophotometer's beam polarized parallel and perpendicular, respectively, to the rubbing direction display high parallel dichroism for the absorption band of azobenzene mesogens at around 365 nm and the absorption bands of P3HT in the 450–650 nm region. LC molecules absorb at wavelengths below 300 nm and their concentrations are too high to allow their anisotropic absorptions to be observed. The polarized absorption spectra indicate that both azobenzene mesogens on the PAzoMA block

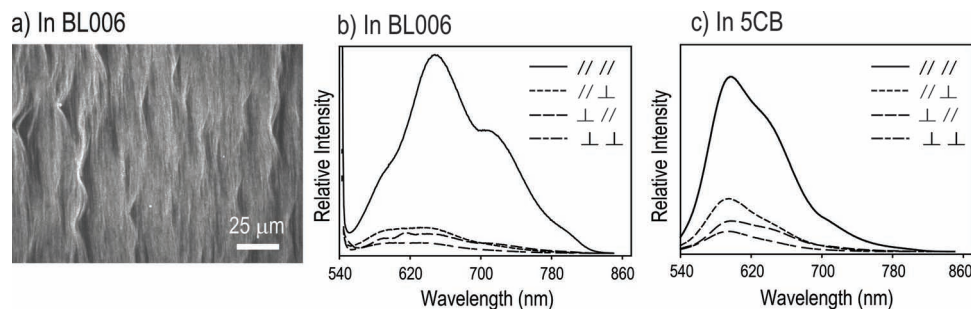


**Figure 2.** a) Fluorescence microscope image of nanofibrils and b,c) polarized fluorescence emission spectra ( $\lambda_{\text{ex}} = 520$  nm) of the nanofibrils recorded at room temperature with different configurations of excitation and detection polarizations. The first and the second symbol indicate the excitation and the detection polarization, respectively, with respect to the rubbing direction.

and the P3HT main chain are oriented parallel to the fibrils. While it is no surprise to see azobenzene mesogens oriented in the same direction as the LC director,<sup>[14]</sup> the observation that P3HT chains are aligned parallel to the fibril growing direction is in sharp contrast with the known nanowires or nanofibers of polythiophenes.<sup>[3,15]</sup> From the absorption spectra, the appearance of three absorption maxima of P3HT at  $\approx 510$ , 550 and 610 nm indicates ordered stacking of P3HT chains inside the fibrils. Of them, the 610 nm band, arising from the interchain  $\pi$ - $\pi$  interaction between stacked thienyl backbones, can be used to monitor the disorder-order transition of P3HT chains accompanying the aggregation process.<sup>[8]</sup> Therefore, for the two systems, we recorded their polarized absorption spectra on cooling from the isotropic state to room temperature and measured the change in absorbance of the 610 nm band,  $A = (A_{\parallel} + 2A_{\perp})/3$ , as well as the change in order parameter,  $S = (A_{\parallel} - A_{\perp})/(A_{\parallel} + 2A_{\perp})$ , of stacked P3HT chains,  $A_{\parallel}$  and  $A_{\perp}$  being the absorbance with parallel and perpendicular polarization, respectively. With both LCs, in the isotropic state, BCP chains appear to be dissolved with disordered P3HT since no absorption band at 610 nm is observable. On cooling, in BL006 (Figure 1b), the 610 nm band emerges at  $\approx 80$  °C, in the nematic phase of the LC host. The absorption intensity increases with decreasing the temperature, reflecting the continuous aggregation of BCP chains and the formation of an increased amount of fibrils. The change in the order parameter, which is a measure of the macroscopic orientation, almost mirrors the change in absorbance. This implies that the disorder-order transition takes place with P3HT chains oriented along the LC director, resulting in a macroscopic orientation of nanofibrils from the beginning of the aggregation. Likewise, in 5CB, the macroscopic orientation of P3HT chains also occurs concomitantly with the formation of fibrils. However, in the latter case, the disorder-order transition occurs at a lower temperature, around 50 °C. Considering that on cooling, the aggregation of BCP chains begins when the P3HT block becomes insoluble while the PAzoMA block remains soluble in the LC solvent, many factors could contribute to determine the temperature at which this process takes place, such as the solubility of each block in the LC, the used BCP concentration and the cooling rate.

Although BCP self-assembly in a block-selective LC solvent is known,<sup>[20]</sup> we performed control tests to confirm the role of the LC-soluble PAzoMA block and the necessity of using an

anisotropic LC environment in producing the oriented nanofibrils of P3HT. In one test, a mixture of BL006 with 2% of P3HT homopolymer (the same P3HT block as in the BCP) was prepared under the same conditions and on cooling, P3HT precipitated in the form of large irregularly-shaped aggregates. In a second experiment, a mixture of 2% BCP in BL006 was introduced into a glass cell whose polyimide surfaces are not rubbed. After cooling to room temperature, BCP aggregates were found to “copy” the LC texture and be located in the defects regions, resulting in no macroscopic orientation of P3HT chains. Therefore, the observed fibrils must originate from the BCP self-assembly in a block-selective and anisotropic solvent. In other words, the aggregation of P3HT chains develops under influence of PAzoMA chains that interact with the oriented LC host. The results for the above experiments are given in Supporting Information (Figures S1,S2).

The oriented nanofibrils of P3HT exhibit highly polarized emission of photoluminescence. Figure 2a shows a fluorescence microscope image of the nanofibrils in BL006. Figure 2b,c are the polarized emission spectra of P3HT upon 520 nm excitation, recorded with the BCP in BL006 and 5CB, respectively. The polarization ratio of photoluminescence can be calculated from different excitation and detection configurations at the emission wavelength maxima.<sup>[21]</sup> We measured two most relevant ratios:  $R_1 = I_{\parallel\parallel}/I_{\perp\perp}$  and  $R_2 = I_{\parallel\perp}/I_{\perp\parallel}$ , where  $I$  is the fluorescence intensity at the peak wavelength, the first index is the orientation of the excitation polarization relative to the rubbing direction and the second index is the orientation of the detection polarization relative to this reference direction. For the nanofibrils formed in BL006 (Figure 2b), the emission spectra yield  $R_1 = 8.8, 21.1, \text{ and } 38.1$ , and  $R_2 = 3.7, 8.2, \text{ and } 15$  for the emission maxima at 596, 648, and 710 nm, respectively. By contrast, with 5CB (Figure 2c), the nanofibrils give rise to  $R_1 = 8.7, 12.6, \text{ and } 19.7$ , and  $R_2 = 3.3, 4.5, \text{ and } 7.8$  at the same emission peaks. In terms of relative intensity, the emission at  $\approx 648$  nm dominates in BL006, while the emission at  $\approx 596$  nm is the most prominent in 5CB. Regarding the anisotropy, the emission at the longest wavelengths around 710 nm, originating from polythiophene chains in an ordered crystalline state, is the most important in both LCs; but the anisotropy of all emission peaks appear to be greater in BL006 than in 5CB. These results imply some difference in the order and organization of P3HT chains inside the fibrils formed in the two different LCs.



After removal of the LC solvent, oriented fibrils could retain on the substrate surface. Although the LC extraction process, understandably, could alter the state of fibrils, substantial anisotropy in absorption and emission of P3HT was still observed (Figure S3, Supporting Information).

Now, the question is how P3HT chains are organized in the nanofibrils. The polarized absorption and emission spectra of the fibrils in both BL006 and 5CB indicate unambiguously that P3HT chain backbones are aligned along, not normal, to the fibrils. This organization is unusual and intriguing for polythiophenes because, as mentioned above, in their nanofibers or nanowires formed via aggregation in solution or nematic LCs,<sup>[3,8,15]</sup> the  $\pi$ - $\pi$  stacking direction of conjugated polythiophene chains determines the nanofibre or nanowire growing direction so that chain backbones are normal to the fibers. The distinct feature of our BCP self-assembly in LCs is that the aggregation (or disorder-order transition) of P3HT is not only governed by its solubility in the LC solvent, but also dictated by the more soluble and orienting PAzoMA block, to which P3HT is connected. Moreover, the absorption spectra of the fibrils (Figure 1) clearly indicate that P3HT chains inside the nanofibrils are ordered giving rise to the two absorption bands at longer wavelengths (550 and 610 nm) associated with an increased chain conjugation length and interchain  $\pi$ - $\pi$  interaction. And judging from the relative absorption intensity of these two bands, the degree of order of P3HT chains inside the nanofibrils is high and comparable to the nanowires formed through solution aggregation.<sup>[8]</sup>

We performed more characterizations in order to get some insight into the self-assembly process and the structure of the nanofibrils. On the one hand, we dissolved a very small amount of BCP in 5CB (0.05 wt%) and cooled the mixture to room temperature under the same conditions. After extracting 5CB in THF, the cell was carefully opened and what remained on the surface was examined with SEM. As seen in Figure 3a, worm-like micellar aggregates with an average width of about 190 nm and length of 1.4  $\mu$ m were observed, suggesting that the aggregation of P3HT-*b*-PAzoMA in LCs tends to form cylindrical micelles. At higher BCP concentrations, such micellar aggregates could condense or coalesce to form the observed fibrils, which are reminiscent of the fibrous aggregates of small-molecule gelators in LCs.<sup>[22,23]</sup> On the other hand, using the mixture of 2% BCP in BL006, after removal of the LC solvent, we used a razor to scratch the surface to collect fibrils and deposited them on a thin slide for X-ray diffraction (XDR) measurements

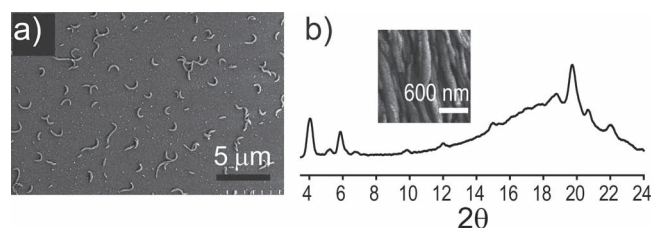


**Figure 3.** a) SEM image of self-assembled aggregates (0.05% of BCP in 5CB). b) X-ray diffraction profile of fragmented nanofibrils scratched from the glass cell surface after extraction of BL006. The inset is a SEM image of the nanofibrils before being removed from the surface.

(the thick glass plate of the cell is non-transparent to X-ray). Figure 3b shows the diffraction pattern recorded with the collected sample. The inset shows a SEM image of nanofibrils after LC solvent removal and prior to scratching. Despite a number of small peaks that may arise from noise, non-removed LC or scratched coating layers on the glass (ITO and polyimide), the prominent diffraction peaks in the  $2\theta$  region of  $4$ – $6^\circ$  can clearly be assigned to ordered structure of the nanofibrils. The peak at  $2\theta = 4.01^\circ$  corresponds to a  $d$  spacing of 22 Å arising from the smectic phase formed by azobenzene mesogens on PAzoMA.<sup>[14]</sup> The peak at  $2\theta = 5.89^\circ$  reveals a  $d$  spacing of 15 Å that is the distance between thienyl backbones separated by hexyl side chains. It is noted that this value is smaller than the  $d$  spacing of 16.5 Å observed for the same BCP microphase-separated in the solid state,<sup>[14]</sup> suggesting an increased interdigitation of the hexyl side chains in the oriented fibrils. The overlapping peaks at around  $2\theta = 20^\circ$  are reflections of the distances between P3HT chains in the  $\pi$ - $\pi$  stacking direction and, mostly, between liquidlike mesogenic moieties within smectic layers of PAzoMA.

Taking into consideration all experimental evidence, the plausible organization of BCP chains in the self-assembled nanofibrils is schematically depicted in Figure 4. On cooling, when P3HT blocks become insoluble in either BL006 or 5CB, they start to aggregate. Being subjected to the influence of surface-oriented LC molecules and mesogenic groups on PAzoMA, like PQT12<sup>[15]</sup> and other rigid  $\pi$ -conjugated polymers,<sup>[24–26]</sup> it is likely that aggregating P3HT chains are already oriented in the same direction as the LC host and mesogenic groups on PAzoMA. This explains why P3HT chain orientation is observed at the beginning of the disorder-order transition (Figure 1). Since the content of P3HT in the BCP is much smaller than PAzoMA,

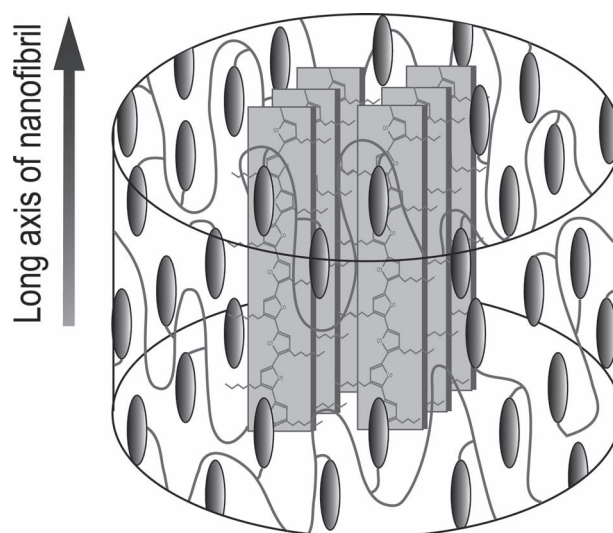


**Figure 4.** Schematic illustration of oriented P3HT chains and mesogenic side groups of the liquid crystalline polymer in the self-assembled nanofibrils (oriented molecules of the liquid crystal host are not shown for simplicity). The unusual feature of this organization is the same direction for oriented P3HT chains and the long axis of nanofibrils, as the  $\pi$ - $\pi$  stacking of P3HT chains cannot grow laterally due to surrounding liquid crystalline polymer.

aggregated P3HT chains should be surrounded and, thus, confined by PAzoMA whose mesogenic side groups are oriented along the LC director. Because of this confinement, P3HT chain packing cannot grow along the  $\pi$ - $\pi$  stacking direction, resulting in P3HT chain orientation parallel to the long axis of formed nanofibrils. Despite the BCP-induced confinement that limits the number of P3HT chains packed normal to the fibrils, the extent of order of aggregated P3HT chains remains high (Figure 1,2). The exact organization of P3HT chains inside the fibrils is unclear at this time. Considering the diblock copolymer structure, some sort of chain folding at the interface of the two blocks may occur to allow or facilitate the alignment of P3HT chains with the mesogenic groups on PAzoMA. In any event, the structure of the self-assembled nanofibrils is determined by a complex interplay between anisotropic intermolecular interactions and LC-phobic interactions (insolubility of P3HT in LCs).

Finally, it is worth being noted that with the used BCP, its concentration in the LC solvent was kept low (below about 5%) to ensure a good solubility in the isotropic state. At this level of BCP concentrations, the method cannot produce large amounts of oriented fibrils. However, all these parameters have not been optimized in the present study. Future work may design BCPs with an improved solubility of the LCP block in nematic LCs, which allows the BCP concentration to be increased. Various lengths of the conjugated polymer and the LCP could also be investigated to determine the effect on the self-assembly process and formation of oriented nanofibrils. Moreover, using, for example, a photo-cleavable junction between the two blocks,<sup>[27–29]</sup> it may be possible to isolate fibrous aggregates of  $\pi$ -conjugated polymers from the non-conducting LCP. These perspectives suggest that it is of great interest to further develop this method for preparing macroscopically oriented nanofibrils of  $\pi$ -conjugated semiconducting polymers.

### 3. Conclusions

We reported a novel and general approach for preparing macroscopically oriented nanofibrils of  $\pi$ -conjugated polymers. It consists in making a BCP comprised of the conjugated polymer of interest, which should be insoluble (or less soluble) in a LC solvent, and a LC polymer, which should be soluble (or more soluble) in it, and exploiting self-assembly of the BCP in a block-selective and oriented nematic LC. With P3HT-*b*-PAzoMA, we found that such self-assembly in different LCs could lead to the formation of highly oriented nanofibrils of regioregular P3HT that display highly anisotropic absorption and polarized photoluminescence emission. To our knowledge, this is the first self-assembly-based method that results in nanofibrils in which P3HT chains are oriented along the fibrils' long axis.

### 4. Experimental Section

Details on the used characterization techniques and the results of control experiments are presented in the Supporting Information.

### Supporting Information

Supporting Information is available from the Wiley Online Library or from the author.

### Acknowledgements

The authors acknowledge financial support from the Natural Sciences and Engineering Research Council of Canada (NSERC) and le Fonds québécois de la recherche sur la nature et les technologies de Québec (FQRNT). Y.Z. is a member of FQRNT-funded CSACS, CQMF, and FRQS-funded Centre de recherche clinique Étienne-Le Bel.

Received: July 23, 2012  
Published online: August 17, 2012

- [1] F. J. M. Hoebe, P. Jonkheijm, E. W. Meijer, A. P. H. Schenning, *Chem. Rev.* **2005**, *105*, 1491.
- [2] F. S. Kim, G. Ren, S. A. Jenekhe, *Chem. Mater.* **2011**, *23*, 682.
- [3] J. A. Lim, F. Liu, S. Ferdous, M. Muthukumar, A. L. Briseno, *Mater. Today* **2010**, *13*, 14.
- [4] M. Brinkmann, F. Chandezon, R. B. Pansu, C. Julien-Rabant, *Adv. Funct. Mater.* **2009**, *19*, 2759.
- [5] N. Kiri, E. Jahne, H.-J. Adler, M. Schneider, A. Kiri, G. Gorodyska, S. Minko, D. Jehnichen, P. Simon, A. A. Fokin, M. Stamm, *Nano. Lett.* **2003**, *3*, 707.
- [6] S. Samitsu, T. Shimomura, S. Heike, T. Hashizume, K. Ito, *Macromolecules* **2008**, *41*, 8000.
- [7] D. H. Kim, Y. D. Park, Y. Jang, S. Kim, K. Cho, *Macromol. Rapid Commun.* **2005**, *26*, 834.
- [8] M. He, L. Zhao, J. Wang, W. Han, Y. Yang, F. Qiu, Z. Lin, *ACS Nano* **2010**, *6*, 3241.
- [9] X. Zhang, A. G. MacDiarmid, A. S. K. Manohar, *Chem. Commun.* **2005**, 5328.
- [10] D. Li, A. Babel, S. A. Jenekhe, Y. Xia, *Adv. Mater.* **2004**, *16*, 2062.
- [11] B. W. Maynor, S. F. Filocamo, M. W. Grinstaff, J. Liu, *J. Am. Chem. Soc.* **2002**, *124*, 522.
- [12] J. Liu, E. Shenina, T. Kowalewski, R. D. McCullough, *Angew. Chem.* **2002**, *114*, 339.
- [13] B. W. Boudouris, C. D. Frisbie, M. A. Hillmyer, *Macromolecules* **2010**, *43*, 3566.
- [14] D. Han, X. Tong, Y. Zhao, Y. Zhao, *Angew. Chem. Int. Ed.* **2010**, *49*, 9162.
- [15] S. Samitsu, Y. Takanishi, J. Yamamoto, *Macromolecules* **2009**, *42*, 4366.
- [16] I. D. Tevis, L. C. Palmer, D. J. Herman, I. P. Murray, D. A. Stone, S. I. Stupp, *J. Am. Chem. Soc.* **2011**, *133*, 16486.
- [17] E. K. Schillinger, E. Mena-Osteritz, J. Hentschel, H. G. Börner, P. Bauerle, *Adv. Mater.* **2009**, *21*, 1562.
- [18] A. P. H. J. Schenning, A. F. M. Kilbinger, F. Biscarini, M. Cavallini, H. J. Cooper, P. J. Derrick, W. J. Feast, R. Lazzaroni, Ph. Leclère, L. A. McDonnell, E. W. Meijer, S. C. J. Meskers, *J. Am. Chem. Soc.* **2002**, *124*, 1269.
- [19] T. Yasuda, K. Kishimoto, T. Kato, *Chem. Commun.* **2006**, 3399.
- [20] W. Shen, K. Zhang, J. A. Kornfield, D. A. Tirrell, *Nat. Mater.* **2006**, *5*, 153.
- [21] F. D. Stasio, P. Korniyuk, S. Brovelli, P. Uznanski, S. O. McDonnell, G. Winroth, H. L. Anderson, A. Tracz, F. Cacialli, *Adv. Mater.* **2011**, *23*, 1855.
- [22] T. Kato, N. Mizoshita, K. Kishimoto, *Angew. Chem. Int. Ed.* **2006**, *45*, 38.
- [23] X. Tong, Y. Zhao, *Adv. Mater.* **2003**, *15*, 1431.
- [24] A. Ohira, T. M. Swager, *Macromolecules* **2007**, *40*, 19.
- [25] J. Hoogboom, T. M. Swager, *J. Am. Chem. Soc.* **2006**, *128*, 15058.
- [26] A. Tcherniak, D. Solis Jr., S. Khatua, A. A. Tangonan, T. R. Lee, S. Link, *J. Am. Chem. Soc.* **2008**, *130*, 12262.
- [27] M. Kang, B. Moon, *Macromolecules* **2009**, *42*, 455–458.
- [28] J. M. Schumers, J. F. Gohy, C. A. Fustin, *Polym. Chem.* **2010**, *1*, 161.
- [29] P. Theato, *Angew. Chem. Int. Ed.* **2011**, *50*, 5804.